



Published in final edited form as:

Ann Surg Oncol. 2013 December ; 20(0 3): S739–S746. doi:10.1245/s10434-013-3318-6.

Overexpression of Membrane Proteins in Primary and Metastatic Gastrointestinal Neuroendocrine Tumors

Jennifer C. Carr, MD^{#1}, Scott K. Sherman, MD^{#1}, Donghong Wang, MS¹, Fadi S. Dahdaleh, MD¹, Andrew M. Bellizzi, MD², M. Sue O’Dorisio, MD, PhD³, Thomas M. O’Dorisio, MD⁴, and James R. Howe, MD¹

¹Department of Surgery, University of Iowa Carver College of Medicine, Iowa City, IA

²Department of Pathology, University of Iowa Carver College of Medicine, Iowa City, IA

³Department of Pediatrics, University of Iowa Carver College of Medicine, Iowa City, IA

⁴Department of Internal Medicine, University of Iowa Carver College of Medicine, Iowa City, IA

These authors contributed equally to this work.

Abstract

Background—Small bowel and pancreatic neuroendocrine tumors (SBNETs and PNETs) are rare tumors whose incidence is increasing. Drugs targeting the somatostatin receptor are beneficial in these tumors. To identify additional cell-surface targets, we recently found receptors and membrane proteins with gene expression significantly different from adjacent normal tissues in a small number of primary SBNETs and PNETs. We set out to validate these expression differences in a large group of primary neuroendocrine tumors and to determine whether they are present in corresponding liver and lymph node metastases.

Methods—Primary SBNETs and PNETs, normal tissue, nodal, and liver metastases were collected and mRNA expression of six target genes was determined by quantitative PCR. Expression was normalized to *GAPDH* and *POLR2A* internal controls, and differences as compared to normal tissue were assessed by Welch’s *t* test.

Results—Gene expression was determined in 45 primary PNETs with 20 nodal and 17 liver metastases, and 51 SBNETs with 50 nodal and 29 liver metastases. Compared to normal tissue, the oxytocin receptor (*OXTR*) showed significant overexpression in both primary and metastatic SBNETs and PNETs. Significant overexpression was observed for *MUC13* and *MEP1B* in PNET primary tumors, and for *GPR113* in primary SBNETs and their metastases. *SCTR* and *ADORA1* were significantly underexpressed in PNETs and their metastases. *OXTR* protein expression was confirmed by immunohistochemistry.

Conclusions—*OXTR* is significantly overexpressed relative to normal tissue in primary SBNETs and PNETs, and this overexpression is present in their liver and lymph node metastases, making *OXTR* a promising target for imaging and therapeutic interventions.

Small bowel and pancreatic neuroendocrine tumors (SBNETs and PNETs) are rare tumors with increasing incidence that present with metastases in over 50 % of cases.^{1–2} Although surgery is the most effective treatment for these tumors, hormone therapy with somatostatin

analogues (SSAs) can curtail symptoms and is associated with significantly improved progression-free survival.³⁻⁴ SSAs are synthetic derivatives of the endogenous hormone somatostatin and include octreotide, lanreotide, and pasireotide. They bind and activate one or more of five human somatostatin receptor (SSTR) subtypes.⁵ Although SSAs show efficacy in functional and nonfunctional tumors and achieve stable disease in >80 % of cases, the disease of most patients eventually progresses and demonstrates increasing SSA resistance over time.⁶⁻⁷ To address late treatment failure, second-line SSAs have binding affinities broadened from the standard SSTR subtype, SSTR2, to those not as well recognized by first-line drugs, such as SSTR1, 3, and 5.⁵ Yet in a recent phase II trial, 88 % of patients with octreotide-resistant disease failed to improve after treatment with pasireotide, a drug with expanded SSTR subtype affinity.⁵ The diminishing returns of new drugs targeting SSTRs demonstrate that further improvement in neuroendocrine tumor (NET) treatment requires novel cell-surface receptor targets.

An ideal receptor target would display features that underlie the success of SSTR-based treatments: high receptor expression in tumor tissue with low expression in background normal tissue. Such differential expression allows ligands binding the SSTR to selectively localize to tumors. Distinct from the antiproliferative effects achieved by activating SSTRs, radioisotopes linked to SSAs use SSTRs to selectively accumulate at tumor tissues, which permits SSTR-based radioimaging and peptide-receptor radionuclide treatment (PRRT) of NETs.⁸⁻¹¹

Several potential target receptors were recently identified by our group on the basis of early experiments measuring gene expression in SBNETs and PNETs using G-protein-coupled-receptor (GPCR) and exon microarrays.¹² In a limited number of primary tumors ($n = 26$), these arrays revealed significant overexpression of over 50 genes compared to normal tissues. Although these investigations aimed to identify genes with different expression in tumors of small bowel versus pancreatic origin, the GPCR arrays' demonstration of significant upregulation of the SSTR2 receptor in both SBNETs and PNETs led us to hypothesize that these data could point to additional receptors useful for NET imaging and therapy. We further hypothesized that as a result of variation in expression of individual genes across tumor specimens, it would be necessary to test expression in a large sample of primary tumors to ensure validity. Finally, for a gene target to be clinically useful, metastatic tissues should have expression profiles similar to primary tumors. We therefore set out to determine expression of six target genes identified from our pilot studies across a much larger group of primary tumor specimens and their associated metastases.

METHODS

Patients and Tumors

Tumors, adjacent normal tissue, lymph nodes, and liver metastases were collected at surgery under an institutional review board–approved protocol with informed consent. Tissues were preserved in RNAlater solution (Life Technologies, Grand Island, NY, USA). RNA was recovered, and quantitative PCR (qPCR) was performed as described.¹² Briefly, total RNA was recovered by the Trizol method and reverse transcribed into cDNA, and triplicate qPCR was performed on a StepOnePlus Real-Time PCR or 7900 HT-Fast RT-PCR System using TaqMan primers and reagents (Life Technologies). Target genes were chosen from pilot GPCR and exon expression array experiments as described, and included G-protein-coupled receptor 113 (*GPR113*; Hs00542378_m1); oxytocin receptor (*OXTR*; Hs00168573_m1); secretin receptor (*SCTR*; Hs01085380_m1); adenosine-A1 receptor (*ADORA1*; Hs00379752_m1); meprin-A-beta receptor (*MEP1B*; Hs00195535_m1); and mucin-13, cell-surface-associated protein (*MUC13*; Hs00217230_m1). Glyceraldehyde-3-phosphate

dehydrogenase (*GAPDH*; Hs02758991_g1) and polymerase (RNA) II polypeptide-A (*POLR2A*; Hs00172187_m1) served as internal control genes.¹²

Data Analysis

Mean threshold cycles (C_t) for each target were normalized to expression of internal control genes. Over- and underexpression were determined by the $\Delta\Delta C_t$ method ($\Delta\Delta C_{t(\text{Gene})} = \text{primary or metastatic tumor expression minus normal small bowel or pancreas tissue expression}$).¹³ Fold changes were calculated as $2^{-\Delta\Delta C_t}$. Welch's *t* test compared mean $\Delta\Delta C_t$ values with significance at $p < 0.01$ as a result of multiple comparisons (R v.2.15.2, Vienna, Austria).

Immunohistochemistry

Immunohistochemistry (IHC) was performed using goat polyclonal antibody raised against a C-terminus human OXTR (sc-8102; Santa Cruz Biotechnology, Santa Cruz, CA, USA). Four-millimeter sections were deparaffinized, rehydrated, and subjected to heat-induced epitope retrieval at 125 °C for 5 min. After incubation with primary antibody for 60 min at room temperature, the Dako Envision Kit (Dako, Carpinteria, CA, USA) was used for detection and slides were lightly counterstained with hematoxylin. Slides were scored as 0 (no staining), 1+ (faint/barely perceptible), 2+ (moderate), or 3+ (strong) by our pathologist (AMB).

RESULTS

Gene Expression in Primary Tumors

qPCR was performed in 51 primary SBNETs (with 29 liver and 50 nodal metastases) and in 45 primary PNETs (with 17 liver and 20 nodal metastases) and their adjacent normal tissues. In primary SBNETs, four genes showed significantly different expression in tumors compared to normal tissues (Table 1, $p < 0.01$). *SCTR* and *MEP1B* were significantly underexpressed in primary SBNETs, with -2.7 - and -5.7 -fold lower expression, respectively. Significant overexpression of 9.9- and 90.5-fold was found for *GPR113* and *OXTR*. This dramatic overexpression of *GPR113* and *OXTR* mRNA in primary tumors compared to normal background tissues revealed these two receptors as promising targets in SBNETs.

In primary PNETs, five genes had significantly different expression levels compared to normal tissues (Table 2, $p < 0.01$). *ADORA1* and *SCTR* showed significant underexpression in primary PNETs, with -9.5 - and -23.1 -fold lower expression, respectively. Unlike SBNETs, in PNET primary tumors, *GPR113* showed no significant expression difference compared to normal tissues (2.2-fold, $p = 0.012$). *MEP1B*, *MUC13*, and *OXTR* were significantly overexpressed in PNET primary tumors, with 21.9-, 6.9-, and 15.2-fold increased expression compared to normal tissues, respectively. From these levels of overexpression, we conclude that *MEP1B*, *MUC13*, and *OXTR* are encouraging gene targets in PNET primary tumors. *OXTR*'s high fold overexpression and its overexpression in both SBNET and PNET primary tumors makes it the most attractive therapeutic target of the group.

Expression in Metastases

Expression compared to normal tissues of these six target genes was measured in nodal and liver metastases associated with these primary tumors. The significant underexpression observed for *ADORA1* and *SCTR* in PNET primary tumors was also present in PNET nodal and liver metastases, while underexpression of *SCTR* and *MEP1B* in SBNET primary

tumors was found in SBNET nodal metastases and in liver metastases for *MEP1B* (Tables 1,2).

However, for a cell-surface molecule to function as a selective marker of tumor tissue, thereby making it useful for imaging or PRRT, overexpression in metastatic as well as primary tumor tissues is of greater clinical utility than underexpression. In the genes identified as possible therapeutic targets, overexpression found in primary tumors was present in metastatic tissues as well, and was sometimes more pronounced (Tables 1, 2). Overall, trends of over- or underexpression found in primary tumors were present in metastases for all target genes studied. In SBNETs, *GPR113* was significantly overexpressed in both liver and nodal metastases (31.6- and 109.1-fold, $p < 0.0001$) compared to normal tissues (Fig. 1). In PNETs, *MEP1B* and *MUC13* were significantly overexpressed compared to normal tissues in liver metastases (11.2- and 5.5-fold, $p < 0.01$). Their 9.4- and 5.5-fold overexpression in nodal metastases did not reach significance (Fig. 2). *OXTR* was markedly overexpressed in liver and nodal metastases of both tumor types, with over 15-fold overexpression in PNET metastases and over 90-fold overexpression in SBNET metastases (Figs. 1, 2; $p < 0.0001$). Significant *OXTR* overexpression compared to normal tissue in primary tumors, liver, and lymph node metastases of both SBNETs and PNETs demonstrates its promise as a cell-surface receptor target for novel therapeutic strategies in these tumors.

Evaluation of a Formula to Distinguish SBNET and PNET Primary Tumors

NETs often present with liver metastases of unknown primary, and differences in gene expression between SBNETs and PNETs might be useful in diagnosing the source of the primary tumor.²⁻¹²⁻¹⁴ Observing that SBNETs tended to have a greater difference than PNETs in expression of *OXTR* and *SCTR*, our group previously devised the formula $2^{(C_tSCTR - C_tOXTR)}$ to distinguish tissue samples' primary site on the basis of the Ct expression levels of these genes.¹² Under this formula, a value of >20 indicates an SBNET and a value of <5 indicates a PNET, with intervening values called indeterminate. In early experiments, this formula correctly classified 22 of 26 (84.6 %) primary tumors and 8 of 10 liver metastases.¹² Therefore, we sought to validate this formula with this larger data set.

In 90 primary tumors with complete data, this formula correctly classified 62 tumors (68.9 %) and incorrectly classified 13 (14.4 %), with 17 tumors (18.9 %) being called indeterminate. In 45 liver metastases, 32 were correctly classified (71.1 %), while 5 (11.1 %) were incorrectly classified with 8 (17.8 %) indeterminate. The formula performed slightly better in PNET liver metastases (13 of 17, 76.5 % correct), than SBNET liver metastases (19 of 28, 67.9 % correct). From these results, we conclude that these genes can assist in discriminating neuroendocrine liver metastases of unknown primary source.

Immunohistochemistry

To verify expression of OXTR protein in NETs, we performed IHC on 7 primary SBNETs and 7 PNETs (Fig. 3). All tumors demonstrated OXTR staining, with more pronounced staining in PNETs than in SBNETs (PNETs: four 3+, two 2+, one 1+; SBNETs: six 2+, one 1+). These results confirm that OXTR protein is present in these tumors, as suggested by qPCR.

DISCUSSION

In this study we identified target genes with overexpression compared to normal background tissue in 96 SBNET and PNET primary tumors, and we found that these patterns of gene expression are maintained in 117 nodal and liver metastases. Of these novel target genes,

OXTR is the most promising because of its high level of overexpression in primary tumors, nodal, and liver metastases in both SBNET and PNETs. We furthermore found that a formula to determine the primary site of neuroendocrine liver metastases based on expression of *OXTR* and *SCTR* is more than 70 % accurate, and we verified the presence of protein in 14 primary SBNETs and PNETs. The oxytocin receptor's overexpression compared to normal tissues suggests that it may be a useful receptor target for imaging and therapeutic strategies in NETs.

The oxytocin receptor is a 389-amino acid G-protein-coupled receptor and is activated by the hormone oxytocin.¹⁵ Initially recognized for its role during parturition to stimulate uterine contraction and lactation, *OXTR* has more recently been investigated for its effects on social behavior, including trust and bonding responses, and in autism-spectrum and anxiety disorders.¹⁵⁻¹⁶ A number of malignant tissues express *OXTR*, including cancers of the breast, brain, reproductive system, colon, and lung.¹⁷⁻¹⁸

The nine-residue oxytocin peptide was first synthesized in 1954 and is widely used in obstetrics to promote labor, while *OXTR*-antagonists such as atosiban serve as tocolytics.¹⁵ Multiple drugs binding *OXTR* are available, making study of the receptor's effect on tumor cells possible.¹⁵ The effects of *OXTR* ligands vary by cellular context. Oxytocin promotes proliferation and migration of *OXTR*-expressing prostate cancer cell lines PC3 and PC3M, and proliferation of small cell lung cancer cell lines DMS79, H146, and H345.¹⁹⁻²⁰ In breast tumor-derived endothelial cells, treatment with oxytocin increases growth and migration.²¹ In contrast, oxytocin causes growth inhibition in glial cells and neoplastic nerve tissues, certain breast cancers, endometrial tumors, and osteosarcoma cells.²²⁻²³ An explanation for these opposite effects in different cell types rests with *OXTR*'s ability to couple with multiple G proteins, leading to activation of different signal cascades in different settings.²⁴

Consistent with this model, *OXTR* signaling can modulate multiple downstream pathways, including phospholipase C, Map-kinase, and the phosphatidylinositol-3-kinase (PI3K)/Akt pathways.¹⁸ In the colon cancer cell line Caco2BB, the PI3K/Akt response to oxytocin treatment is dose and time dependent. Whereas low-dose oxytocin treatment causes increased PI3K signaling and phospho-Akt, with higher concentrations and longer treatments, phospho-Akt decreases.¹⁸ These effects depend on the particular G protein present and on receptor internalization at high oxytocin concentrations.¹⁸ Down-regulation of mTORC1 and an inhibitory effect on translation in response to oxytocin stimulation also occurs.²⁵ Although oxytocin's role is not straightforward in these cells, it is notable that the PI3K/Akt and mTOR pathways are inhibited by *OXTR* in gut cells, as these pathways are important in NETs. The PI3K/Akt pathway has been proposed as a pharmacologic target in NETs on the basis of the observation that blocking the PI3K pathway in pulmonary carcinoid tumors causes reduced growth.²⁶ Similarly, the mTOR inhibitor everolimus has activity against bronchial carcinoids and prolongs progression-free survival in PNETs.²⁷⁻²⁸ Although the pleiotropic effects of *OXTR*-stimulation make prediction of response in SBNETs and PNETs to oxytocin difficult, such evidence linking *OXTR* ligand binding to PI3K/Akt and mTOR inhibition, coupled with our finding of its overexpression in NETs, makes *OXTR* an exciting therapeutic target. Determining the effects of oxytocin on cultured NET cells will be the next step in evaluating this further.

Detectable mRNA by qPCR does not guarantee a translated protein; evidence from our study and others suggests that *OXTR* is present in these NETs. Welch et al. found that tissues in the rat enteric nervous system produce oxytocin and express *OXTR* by RT-PCR, which was confirmed by IHC.²⁹ Interestingly, *OXTR*s are widely expressed in intestinal villi of newborn rats, but by soon after birth, only cells clustering at the crypt-villus junction have *OXTR* staining.²⁹ These *OXTR*-positive cells reside in the expected location of the

enterochromaffin cells from which NETs originate. Together, these results demonstrate a role for oxytocin and its receptor in the gut, suggest that OXTR expression may be specific to neuroendocrine tissues, and support that OXTR protein is present in NET tissues as suggested by qPCR. Our IHC in 7 SBNETs and 7 PNETs shows positive OXTR immunostaining in all tumors examined. That SBNETs, which have higher mRNA expression by qPCR, had less staining than PNETs raises the possibility that additional regulatory mechanisms might modulate OXTR protein levels in these tumors, but positive IHC staining in all tumor tissues studied validates our conclusion from qPCR that OXTR is overexpressed compared to background tissue in these NETs.³⁰

Expression of OXTR by other tissues and the affinity of oxytocin analogues for vasopressin receptors present a potential problem for OXTR-directed drugs.^{15–23} We have demonstrated *OXTR* overexpression in NETs, but it is conceivable that OXTR or vasopressin receptor expression in other tissues could cause false-positive imaging results or bystander tissue effects with PRRT. Although we did not measure gene expression in normal gastrointestinal tissues other than small bowel and pancreas, Roth et al.³¹ studied 45 different tissue types and found underexpression of *OXTR* in normal liver, colon, stomach, and spleen, as well as significant overexpression in brain, bronchus, and female reproductive tissues. Low *OXTR* expression in normal abdominal tissues with high expression in NET tumors supports the potential of OXTR-based tumor imaging. Furthermore, Chini et al.¹⁷ successfully imaged *OXTR*-positive breast tumors in mice with an [¹¹¹In]-DOTA-oxytocin analogue. They noted that their oxytocin analogue can accommodate higher-energy PRRT ligands such as [⁹⁰Y] and [¹⁷⁷Lu], similar to DOTA-octreotide analogues used in NETs, and demonstrated that OXTRs are internalized after ligand binding.¹⁷ Successful tumor imaging with an oxytocin analogue and internalization of the receptor, facilitating radiation delivery directly to the tumor, lend further impetus to development of oxytocin analogues for NET treatment.

At presentation, 50–85 % of SBNETs and PNETs have liver metastases, and liver metastases of unknown primary tumor remain a clinical problem.² In one single-institution series, a primary tumor could not be identified by imaging before surgery in 14 % of patients with NET liver metastases.¹⁴ In this study, we confirmed our earlier observation that differences in *SCTR* and *OXTR* expression can help distinguish between SBNETs and PNETs.¹² However, the accuracy for liver metastases of 71 % in this validation set was lower than the 80 % we reported in our 10 original metastases.¹² This again highlights the importance of validating gene expression findings, and although this accuracy may be insufficient to influence clinical decisions at this time, we continue to identify additional informative genes, which may improve our model's performance.

Two strengths of our study are its large sample size and inclusion of metastases. Gene expression data are susceptible to effects of outlier measurements in small data sets, and small sample sizes are a limitation of most NET gene expression studies.^{32–35} For this reason, our earlier study, with only 15 primary PNETs, failed to identify *OXTR* overexpression as a feature of PNETs, despite its 15-fold overexpression in the present study.¹² Although investigations with small numbers of tumors are useful first steps toward identifying interesting gene targets, the potential of outlying genes to give both false-positive and false-negative results makes confirmation of such findings in larger data sets essential.

Examining metastases is likewise necessary before developing treatments targeting novel receptors. It is increasingly understood that in most cancers, metastases differ from primary tumors by mutations in only a few key genes, yet if these or other “passenger” mutations altered the expression of our target genes in nodal and liver metastases, then these targets might not be useful.³⁶ Our findings confirm that *OXTR* overexpression in primary tumors is

also present in corresponding metastases, meaning that OXTR-directed therapeutics would also be expected to be effective at distant sites of disease.

Acknowledgments

We gratefully acknowledge our patients' generosity. Jennifer C. Carr and Scott K. Sherman were supported by NIH 5T32-CA148062-03.

REFERENCES

1. Yao JC, Hassan M, Phan A, et al. One hundred years after "carcinoid": epidemiology of and prognostic factors for neuroendocrine tumors in 35,825 cases in the United States. *J Clin Oncol.* 2008; 26:3063–72. [PubMed: 18565894]
2. Modlin IM, Oberg K, Chung DC, et al. Gastroenteropancreatic neuroendocrine tumours. *Lancet Oncol.* 2008; 9:61–72. [PubMed: 18177818]
3. Rinke A, Muller HH, Schade-Brittinger C, et al. Placebo-controlled, double-blind, prospective, randomized study on the effect of octreotide LAR in the control of tumor growth in patients with metastatic neuroendocrine midgut tumors: a report from the PROMID Study Group. *J Clin Oncol.* 2009; 27:4656–63. [PubMed: 19704057]
4. Oberg K, Knigge U, Kwekkeboom D, Perren A. Neuroendocrine gastro-entero-pancreatic tumors: ESMO Clinical Practice Guidelines for diagnosis, treatment and follow-up. *Ann Oncol.* 2012; 23(Suppl 7):vii124–30. [PubMed: 22997445]
5. Kvols LK, Oberg KE, O'Dorisio TM, et al. Pasireotide (SOM230) shows efficacy and tolerability in the treatment of patients with advanced neuroendocrine tumors refractory or resistant to octreotide LAR: results from a phase II study. *Endocr Relat Cancer.* 2012; 19:657–66. [PubMed: 22807497]
6. Sideris L, Dube P, Rinke A. Antitumor effects of somatostatin analogs in neuroendocrine tumors. *Oncologist.* 2012; 17:747–55. [PubMed: 22628056]
7. Hofland LJ, Lamberts SW. The pathophysiological consequences of somatostatin receptor internalization and resistance. *Endocr Rev.* 2003; 24:28–47. [PubMed: 12588807]
8. Krenning EP, Kwekkeboom DJ, Bakker WH, et al. Somatostatin receptor scintigraphy with [¹¹¹In-DTPA-d-Phe1]- and [¹²³I-Tyr3]-octreotide: the Rotterdam experience with more than 1000 patients. *Eur J Nucl Med.* 1993; 20:716–31. [PubMed: 8404961]
9. Gabriel M, Decristoforo C, Kendler D, et al. 68 Ga-DOTA-Tyr3-octreotide PET in neuroendocrine tumors: comparison with somatostatin receptor scintigraphy and CT. *J Nucl Med.* 2007; 48:508–18. [PubMed: 17401086]
10. Zaknun JJ, Bodei L, Mueller-Brand J, et al. The joint IAEA, EANM, and SNMMI practical guidance on peptide receptor radionuclide therapy (PRRNT) in neuroendocrine tumours. *Eur J Nucl Med Mol Imaging.* 2013; 40:800–16. [PubMed: 23389427]
11. Dahdaleh FS, Lorenzen A, Rajput M, et al. The value of preoperative imaging in small bowel neuroendocrine tumors. *Ann Surg Oncol.* 2013; 20:1912–7. [PubMed: 23283442]
12. Carr JC, Boese EA, Spanheimer PM, et al. Differentiation of small bowel and pancreatic neuroendocrine tumors by gene-expression profiling. *Surgery.* 2012; 152:998–1007. [PubMed: 23158174]
13. Buckhaults P, Zhang Z, Chen YC, et al. Identifying tumor origin using a gene expression-based classification map. *Cancer Res.* 2003; 63:4144–9. [PubMed: 12874019]
14. Wang SC, Parekh JR, Zuraek MB, et al. Identification of unknown primary tumors in patients with neuroendocrine liver metastases. *Arch Surg.* 2010; 145:276–80. [PubMed: 20231629]
15. Manning M, Misicka A, Olma A, et al. Oxytocin and vasopressin agonists and antagonists as research tools and potential therapeutics. *J Neuroendocrinol.* 2012; 24:609–28. [PubMed: 22375852]
16. Ebstein RP, Knafo A, Mankuta D, Chew SH, Lai PS. The contributions of oxytocin and vasopressin pathway genes to human behavior. *Horm Behav.* 2012; 61:359–79. [PubMed: 22245314]

17. Chini B, Chinol M, Cassoni P, et al. Improved radiotracing of oxytocin receptor-expressing tumours using the new [¹¹¹In]-DOTA-Lys8-deamino-vasotocin analogue. *Br J Cancer*. 2003; 89:930–6. [PubMed: 12942128]
18. Klein BY, Tamir H, Welch MG. PI3K/Akt responses to oxytocin stimulation in Caco2BB gut cells. *J Cell Biochem*. 2011; 112:3216–26. [PubMed: 21732407]
19. Zhong M, Boseman ML, Millena AC, Khan SA. Oxytocin induces the migration of prostate cancer cells: involvement of the Gi-coupled signaling pathway. *Mol Cancer Res*. 2010; 8:1164–72. [PubMed: 20663860]
20. Pequeux C, Breton C, Hendrick JC, et al. Oxytocin synthesis and oxytocin receptor expression by cell lines of human small cell carcinoma of the lung stimulate tumor growth through autocrine/paracrine signaling. *Cancer Res*. 2002; 62:4623–9. [PubMed: 12183418]
21. Cassoni P, Marrocco T, Bussolati B, et al. Oxytocin induces proliferation and migration in immortalized human dermal microvascular endothelial cells and human breast tumor-derived endothelial cells. *Mol Cancer Res*. 2006; 4:351–9. [PubMed: 16778082]
22. Cassoni P, Sapino A, Stella A, Fortunati N, Bussolati G. Presence and significance of oxytocin receptors in human neuroblastomas and glial tumors. *Int J Cancer*. 1998; 77:695–700. [PubMed: 9688301]
23. Cassoni P, Sapino A, Marrocco T, Chini B, Bussolati G. Oxytocin and oxytocin receptors in cancer cells and proliferation. *J Neuroendocrinol*. 2004; 16:362–4. [PubMed: 15089975]
24. Gravati M, Busnelli M, Bulgheroni E, et al. Dual modulation of inward rectifier potassium currents in olfactory neuronal cells by promiscuous G protein coupling of the oxytocin receptor. *J Neurochem*. 2010; 114:1424–35. [PubMed: 20557424]
25. Klein BY, Tamir H, Hirschberg DL, Glickstein SB, Welch MG. Oxytocin modulates mTORC1 pathway in the gut. *Biochem Biophys Res Commun*. 2013; 432:466–71. [PubMed: 23410756]
26. Pitt SC, Chen H, Kunnimalaiyaan M. Phosphatidylinositol 3-kinase-Akt signaling in pulmonary carcinoid cells. *J Am Coll Surg*. 2009; 209:82–8. [PubMed: 19651067]
27. Oberg KE, Casanovas O, Castano JP, et al. Molecular pathogenesis of neuroendocrine tumors: implications for current and future therapeutic approaches. *Clin Cancer Res*. 2013; 19:2842–9. [PubMed: 23459719]
28. Pavel ME, Hainsworth JD, Baudin E, et al. Everolimus plus octreotide long-acting repeatable for the treatment of advanced neuroendocrine tumours associated with carcinoid syndrome (RADIANT-2): a randomised, placebo-controlled, phase 3 study. *Lancet*. 2011; 378:2005–12. [PubMed: 22119496]
29. Welch MG, Tamir H, Gross KJ, Chen J, Anwar M, Gershon MD. Expression and developmental regulation of oxytocin (OT) and oxytocin receptors (OTR) in the enteric nervous system (ENS) and intestinal epithelium. *J Comp Neurol*. 2009; 512:256–70. [PubMed: 19003903]
30. Vogel C, Marcotte EM. Insights into the regulation of protein abundance from proteomic and transcriptomic analyses. *Nat Rev Genet*. 2012; 13:227–32. [PubMed: 22411467]
31. Roth RB, Hevezi P, Lee J, et al. Gene expression analyses reveal molecular relationships among 20 regions of the human CNS. *Neurogenetics*. 2006; 7:67–80. [PubMed: 16572319]
32. Slaby O, Sachlova M, Bednarikova M, et al. Gene expression of somatostatin receptor 4 predicts clinical outcome of patients with metastatic neuroendocrine tumors treated with somatostatin analogs. *Cancer Biother Radiopharm*. 2010; 25:237–43. [PubMed: 20423238]
33. Nakayama Y, Wada R, Yajima N, Hakamada K, Yagihashi S. Profiling of somatostatin receptor subtype expression by quantitative PCR and correlation with clinicopathological features in pancreatic endocrine tumors. *Pancreas*. 2010; 39:1147–54. [PubMed: 20717067]
34. O'Toole D, Saveanu A, Couvelard A, et al. The analysis of quantitative expression of somatostatin and dopamine receptors in gastro-entero-pancreatic tumours opens new therapeutic strategies. *Eur J Endocrinol*. 2006; 155:849–57. [PubMed: 17132755]
35. Posorski N, Kaemmerer D, Ernst G, et al. Localization of sporadic neuroendocrine tumors by gene expression analysis of their metastases. *Clin Exp Metastasis*. 2011; 28:637–47. [PubMed: 21681495]
36. Vogelstein B, Papadopoulos N, Velculescu VE, Zhou S, Diaz LA Jr, Kinzler KW. Cancer genome landscapes. *Science*. 2013; 339:1546–58. [PubMed: 23539594]

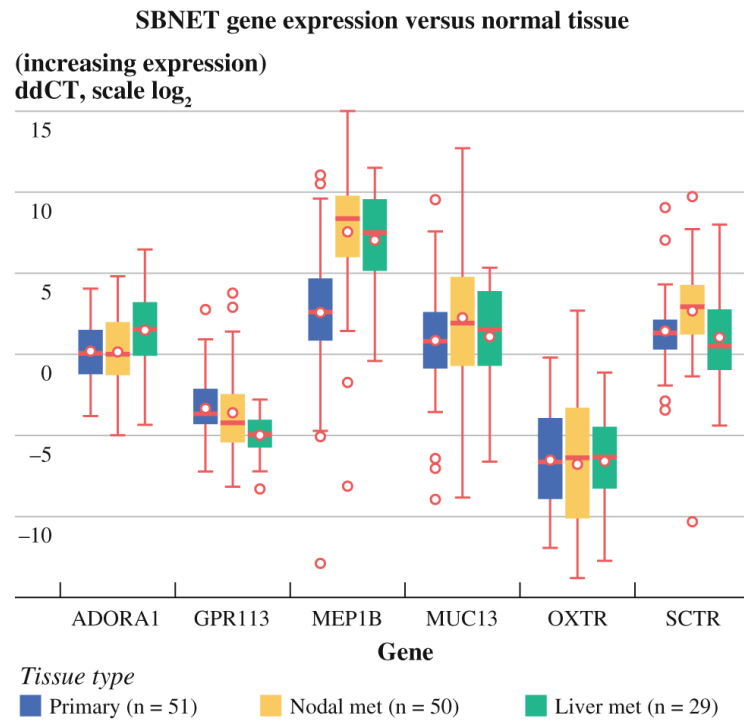


FIG. 1. BNET gene expression versus normal tissue. *GPR113* and *OXTR* are significantly overexpressed in primary tumors and nodal and liver metastases compared to normal small bowel tissue. Expression shown in terms of $\Delta\Delta Ct$ on log scale with *lower numbers* indicating increasing expression. Boxes 25th to 75th percentile of expression, *dot* mean, *bar* median, *whiskers* 1.5*IQR, *open circles* outliers, *dotted line* at 0 expression equal to normal tissue

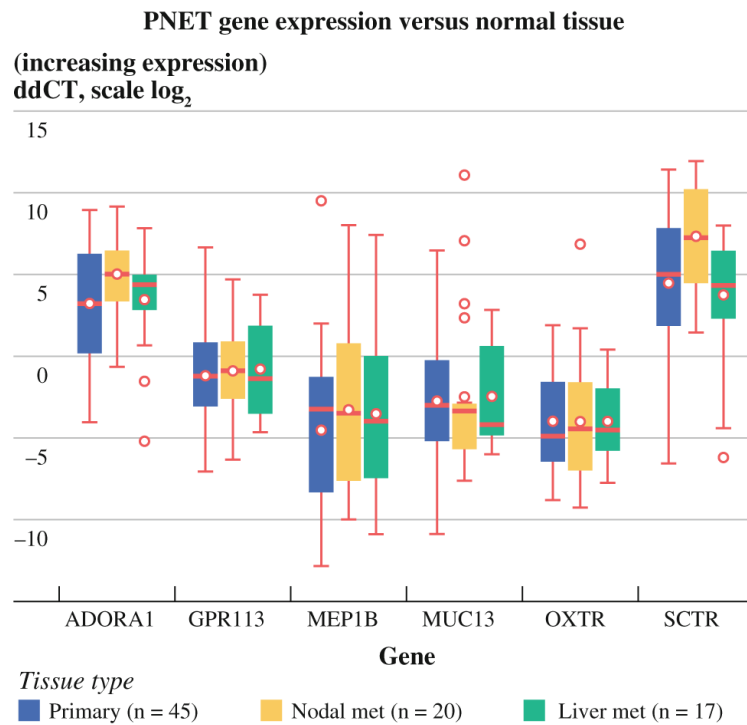


FIG. 2. NET gene expression versus normal tissue. *OXTR* is significantly overexpressed in primary tumors and nodal and liver metastases compared to normal pancreatic tissue. Expression shown in terms of $\Delta\Delta C_t$ on log scale with *lower numbers* indicating increasing expression. *Boxes* 25th to 75th percentile of expression, *dot* mean, *bar* median, *whiskers* 1.5*IQR, *open circles* outliers, *dotted line* at 0 expression equal to normal tissue

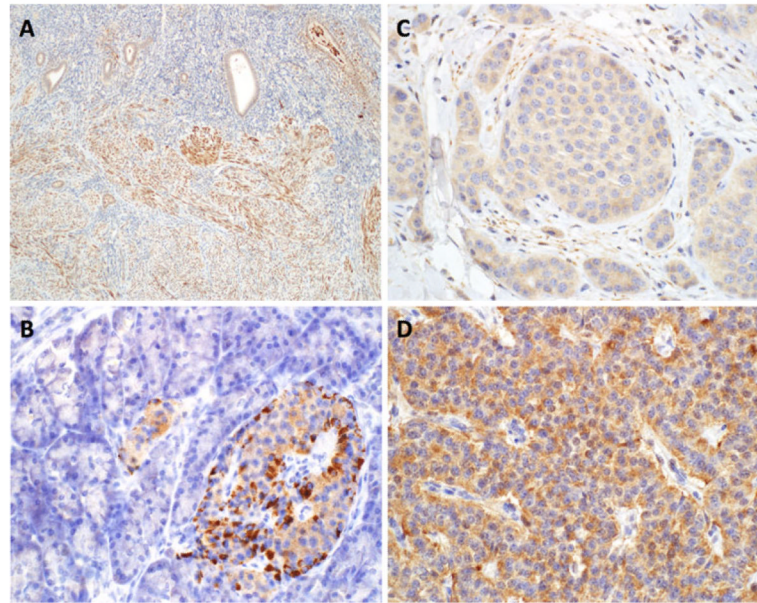


FIG. 3. HC demonstrates detection of oxytocin receptor protein. Shown are images representative of 7 SBNET and 7 PNET samples. **a** Normal endomyometrium positive control (original magnification, $\times 100$) demonstrates 3+ staining in myometrium with 2+ in endometrial glands and 0 in endometrial stroma. **b** Normal pancreas (original magnification, $\times 400$) with 2–3+ staining in normal islets and no staining in acinar parenchyma. **c** SBNET (original magnification, $\times 400$) with 2+ staining in tumor cells. **d** PNET (original magnification, $\times 400$) with 3+ staining in tumor cells

TABLE 1

SBNET gene expression relative to normal tissue

Gene name	Primary tumors (n = 51)		Liver metastases (n = 29)		Nodal metastases (n = 50)	
	Fold change	p value	Fold change	p value	Fold change	p value
<i>ADORA1</i>	-1.1	0.5	-2.8*	0.0017	-1.1	0.7
<i>GPR113</i>	9.9*	2.00E-16	31.6*	2.00E-16	109.1*	4.80E-13
<i>MEP1B</i>	-5.7*	6.88E-05	-135.3*	7.10E-13	-184.8*	2.20E-16
<i>MUC13</i>	-1.8	0.083	-2.1	0.067	-4.6*	0.00076
<i>OXTR</i>	90.5*	2.20E-16	93.7*	1.38E-11	109.1*	4.04E-15
<i>SCTR</i>	-2.7*	1.73E-05	-2.1	0.067	-6.3*	3.51E-07

Listed are expression fold changes and *p* values compared to normal tissue* *p*<0.01 versus normal tissue

TABLE 2

PNET gene expression relative to normal tissue

Gene name	Primary tumors (n = 45)		Liver metastases (n = 17)		Nodal metastases (n = 20)	
	Fold change	p value	Fold change	p value	Fold change	p value
<i>ADORA1</i>	-9.5*	5.12E-07	-11.6*	0.00059	-32.7*	1.59E-07
<i>GPR113</i>	2.2	0.012	1.7	0.33	1.8	0.24
<i>MEP1B</i>	21.9*	1.01E-06	11.2*	0.007	9.4	0.011
<i>MUC13</i>	6.9*	1.61E-05	5.5*	0.007	5.5	0.046
<i>OXTR</i>	15.2*	1.05E-09	15.9*	1.60E-05	15.8*	0.0003
<i>SCTR</i>	-23.1*	3.78E-09	-14.1*	0.003	-162.0*	3.12E-09

Listed are expression fold changes and p values compared to normal tissue

* p<0.01 versus normal tissue